Collapse and revival in the dynamics of a spin with the spin-orbit potential

R. Arvieu*
Institut des Sciences Nucléaires, F 38026 Grenoble Cedex, France

P. Rozmej†
Department of Theoretical Physics, Institute of Physics,
University Maria Curie-Skłodowska, PL 20-031 Lublin, Poland
and Gesellschaft für Schwerionenforschung mbH, Darmstadt, Postfach 11 05 52, 64220 Darmstadt, Germany
(Received 4 May 1994)

We have calculated the time evolution of the density matrix reduced to the spin degree of freedom for a particle in a spherical harmonic oscillator with a constant spin-orbit interaction. We have studied two classes of spatial wave functions in the initial state: pure orbital states $|lm\rangle$ and coherent states. When the initial spin is a pure state, its evolution in time produces a mixed state during a time called the collapse time. This behavior of the spin is similar to that observed in the Jaynes-Cummings model. A similar dynamics is produced for a broad range of geometrical initial conditions for the spin as well as for the wave packet. The system is exactly recurrent, but we have also found the existence of approximate recurrences corresponding to a reversal of the spin direction. We have tentatively applied our result to mimic the evolution of the spin in the H atom. In this case only a few spin-orbit partners play a role and, after a long time, produce a state where the admixture is not complete. The average quantum behavior is always very different from that of a classical particle having a spin as a vector of constant length. The increase of the number $2S+1$ of spin-orbit partners changes the time scale of the collapse by the factor $\sqrt{S}$ and a strong mixing is always observed.

PACS number(s): 03.65.Sq, 03.65.Ge, 32.90.+a

I. INTRODUCTION

Coherent states play a major role in quantum mechanics. Indeed, one of their properties, which is certainly the most appreciated, is that with them one can attempt to bridge the gap between classical and quantum physics. The coherent states of the harmonic oscillator make up a basic tool that can be found in all the textbooks of quantum mechanics or quantum optics [1]. In recent years [2,3] coherent states were constructed for the hydrogen atom and their evolution in time has been shown to present a very beautiful succession of partial recurrences and revivals [3]. It has even been possible to follow the succession of these events experimentally in the case of atomic potassium and rubidium [4]. On the other hand, coherent states were used in a different context: to build up the classical limit of model Hamiltonians which correspond to a large number N of interacting particles. In this limit, called the $1/N$ expansion [5], the number $1/N$ takes the place of the Planck constant. In some of these models, for example, the Lipkin SU(3) model [6,7], the classical dynamics presents regular and chaotic motion within various degrees. A large amount of work has been devoted to the comparison of the results of classical and quantum mechanics on this basis.

It is a major problem to extend these models and theories to cases where spin is present quantum mechanically. In this direction it is important to quote the extensive work that has been made on the Jaynes-Cummings model [8] where a two-level system is coupled to a one-dimensional coherent state. This coupling has been shown to generate Rabi oscillations as well as a suppression of them, called Cummings collapse. This collapse means a situation where the spin is entangled with the electromagnetic field. It does not last forever and one observes a revival of the spin state which separates from the field. This situation is recurrent [9]. When it is analyzed in classical terms, chaos is also observed [10] and one obtains a situation called chaotic Rabi oscillations. The question of quantum irreversibility of this model was raised. It was concluded [11] that the irreversibility could be attributed to nonlinearity leading to chaos. More recently, a second model where spin is also present was considered by Ballentine [12], which consists of a localized spin driven by a polarized beam of spins. Classical and quantum theory have been shown to exhibit a rich variety of dynamical behaviors. The concept of dynamical driving was emphasized by Ballentine to qualify the fact that a system is driven by another dynamical system and not by an external force. This definition could qualify the models already studied by Slosser, Meystre, and Braunstein [13] and also the Jaynes-Cummings model as stressed by Gea-Banacloche [14].

The work that will be described in this article concerns a particle of spin $\frac{1}{2}$ embedded in a spherically symmetric potential with a spin-orbit coupling. We also have here

*Electronic address: arvieu@frcpn11.in2p3.fr
†Electronic address: rozmej@plumcs11.umcs.lublin.pl and tp41@mvs.gsi.de

 ©1995 The American Physical Society

a situation where there is a mutual dynamical driving of the spin degree of freedom by the orbital one. If this problem is treated classically, i.e., if we treat the spin as a classical angular momentum of constant length, the solution is rather elementary for a spherical harmonic oscillator. If the harmonic oscillator is deformed, however, we have proved numerically elsewhere [15] that the spin-orbit coupling is able to produce chaotic orbits and that these orbits belong to manifolds that occupy the phase space with a large dimension of 4, 5, or 6, for example. This deformed model is a simple approximation for Nilsson's model [16], the quantum-mechanical single-particle model that helps to analyze deformed nuclei. Therefore, with this model we have a situation similar to the hydrogen atom in magnetic field, [17] where the classical phase space contains order and chaos, and this is why it deserves a more extensive analysis.

Since the spin-orbit force plays a dominant role in the splitting of the nuclear single-particle levels, both in the spherical and in deformed case, it is an interesting question to analyze to what extent the classical model is valid. This problem will be discussed in what follows only for the spherical case. We want to follow the time evolution of a wave packet that is initially a coherent state of harmonic oscillator times a spin function. First, we show that the equations of motion of the average position, average momentum, and average spin components are the equations followed by one classical particle provided that the spin stays in a pure state at any time. It is therefore crucial to know the reduced spin density matrix, discussed extensively in Ballentine's book [18], as a function of time. Although the evolution operator can be calculated formally, it is not possible to work out the expectation values of the spin components as a function of time in analytic form, as we will show. An analytic form can be calculated, however, for short times. We have also performed a numerical calculation by conveniently using the expansion of the coherent state on the spherical basis derived by Mikhailov [19]. We have obtained the following results. The pure state is exactly recurrent and the period of recurrence is a common multiple of all the quantum periods. However, the spin state is far from being pure in the interval between two recurrences, even for high quantum numbers. An analytical formula valid for short times shows that indeed the spin behavior is far off from this classical behavior. For a large fraction of the period, the state is strongly mixed and the average length of the spin is close to zero to various degrees, depending on the initial direction of the spin. The discussion of these initial conditions is also made and is presented in the most generalized way. The conclusions are somewhat similar to Ballentine's. However, our system is totally different: there is no limit $t \to \infty$ since the system is periodic and we have exact recurrences of the pure state; therefore, we have also some features common with the Jaynes-Cummings model. We have also some features common with an extension of the Jaynes–Cummings model [20] in which the spin interacts nonlinearly with the field by two-photon exchange. Finally, we will also study the effects produced by an increase of the spin which is such that the spin-orbit force is kept constant.

In Sec. VII we will tentatively apply our model for the evolution of the spin in the hydrogen atom in a particular case when the wave packet contains every possible partial wave with the restriction that each partial wave has a unique radial quantum number, the lowest one, $n = l+1$. Under these conditions the spin average decouples from the orbital motion. We have not been able to treat more general cases where such a decoupling does not take place and where studying the spin evolution is an interesting challenge.

II. THE CASE OF ONE CLASSICAL PARTICLE

We start with the simple spherically symmetric harmonic oscillator potential with a frequency ω_0 that is perturbed by a spin-orbit interaction of the form

$$V_s = \kappa\,(\vec{l}\cdot\vec{s})\ . \tag{1}$$

Here $\vec{s}$ is an angular momentum of constant length and κ is a negative coupling constant which scales the spin precession. The orbital angular momentum $\vec{l}$ and the spin vector $\vec{s}$ obey the equations

$$\frac{d\vec{s}}{dt} = \kappa\,(\vec{l}\times\vec{s}) = -\frac{d\vec{l}}{dt}\ , \tag{2}$$

which show that $\vec{j} = \vec{l} + \vec{s}$ is a constant vector while both $\vec{l}$ and $\vec{s}$ rotate around with the classical frequency

$$\omega_{\rm cl} = \kappa\, j\ . \tag{3}$$

The classical model contains five constants of motion: the vector $\vec{j}$, the length L of $\vec{l}$, and the total energy $E = E_0 + \kappa\,(\vec{l}\cdot\vec{s})$. The phase space of this system contains the variables $\vec{r}$ and $\vec{p}$ of the particle as well as the polar angles θ_s, and ϕ_s of the spin vector. The canonical variables associated with the spin are $q_s = \phi_s$, and $p_s = s\cos\theta_s$. There are only four constants of motion in involution E, j, j_z, and l and four degrees of freedom x, y, z, and ϕ_s. Therefore the system is integrable according to Liouville-Arnold theorem [21]. Throughout the rest of the paper only the spin motion will be considered. However, a convenient radial property can be mentioned. In the reference frame, which rotates with the frequency $s\kappa$ around $\vec{s}$, the spin-orbit coupling and the inertial forces cancel and the trajectories are simple ellipses since the force is simply harmonic.

The projection s_z of $\vec{s}$ obeys the equation

$$s_z = \overline{s_z} + (s - \overline{s_z})\ \cos(\omega_{\rm cl} t) \tag{4}$$

if $\vec{s}$ starts at time 0 aligned along Oz. The value of $\overline{s_z}$, depending on the inclination of $\vec{j}$ with respect to Oz, is given by

$$\overline{s_z} = s - s\,\frac{j_\perp}{j}\ . \tag{5}$$

III. THE QUANTUM CASE

In the quantum case also there are four commuting constants of motion E, j^2, j_z, and l^2. Our problem is to compare the evolution in time of the expectation values of $\langle\vec{r}\rangle$, $\langle\vec{p}\rangle$, and $\langle\vec{s}\rangle$ with the classical evolution for general wave packets which are not necessarily characterized by pure quantum numbers.

For $\kappa = 0$ it is well known that the equations are strictly the classical ones and that the wave packet does not spread if it is a coherent state at time zero. Ehrenfest's equations lead, because of the spin-orbit coupling, to averages of products which couple the components of $\vec{s}$ to the components of $\vec{r}$, $\vec{p}$, and $\vec{l}$; for example,

$$i\frac{d\langle s_z\rangle}{dt} = \langle[s_z, H]\rangle = i\kappa\langle s_y l_x - s_x l_y\rangle \ . \tag{6}$$

Here and in the following, s_i, l_i, and j_i are dimensionless. Equation (6) for the evolution of $\langle s_z\rangle$ coincides with Eq. (2) for the classical component of s_z if the factorization of the spin part and of the radial part can be performed at any time:

$$\langle s_y l_x - s_x l_y\rangle = \langle s_y\rangle\langle l_x\rangle - \langle s_x\rangle\langle l_y\rangle \ . \tag{7}$$

In the case of a harmonic oscillator potential the operators involved by the commutators of the Ehrenfest equations are simply $\vec{s}$, $\vec{r}$, $\vec{p}$, or $\vec{l}$ and therefore a closed set of average values is obtained which is identical to the set that is present with the classical equations. Therefore, we can assert that the average values under consideration evolve identically to the classical ones if the spin state is pure at any time. This condition is necessary as well as sufficient. Such a condition that the classical limit is obtained, although there is no decoherence in the dynamics, was previously found and discussed in Ballentine's model [12]. It is a very simple matter to prove that this result takes place in our model.

Obviously the best tool to analyze the validity of condition (7) is the density matrix reduced to the spin degree of freedom. There is an extensive discussion of such a tool in the book by Ballentine [18]. Let us just remind the reader that it can be applied to our system, which is composed of an orbital part and a spin part that are generally correlated due to the term (1). In the following the total system will always be a pure state. To be specific let us denote the wave packet at time zero as $|\zeta\rangle \otimes |s\rangle = |\zeta, s\rangle_0$. In the following $|\zeta\rangle$ will be either a harmonic oscillator coherent state or a simple eigenstate $|lm\rangle$, while $|s\rangle$ will be a spinor pointing in an arbitrary but fixed direction. At time t the system has evolved to a new wave packet

$$|\zeta, s\rangle_t = U(t)\,|\zeta, s\rangle_0 \ . \tag{8}$$

The reduced density matrix ρ_s that we will use is then defined as

$$\rho_s = \mathrm{Tr}_{(nlm)}\{|\zeta, s\rangle_t\ {}_t\langle\zeta, s|\} \ , \tag{9}$$

where (nlm) means that the trace operates only on the radial and angular variables. A second reduced density matrix ρ_r can be defined by summing over the spin space only. Then Ballentine has shown that if ρ_s is a pure state, it is a factor of the total density matrix ρ such that $\rho = \rho_s \otimes \rho_r$. This is why the factorization (7) is possible. It is well known that ρ_s can be expressed in terms of the vector $\vec{a} = \langle\vec{\sigma}\rangle$ as

$$\rho_s = \tfrac{1}{2}(1 + \vec{a}\cdot\vec{\sigma}) \ . \tag{10}$$

As we specialize to the case of spin $\frac{1}{2}$, here and in the following $\vec{\sigma}$ represents the usual Pauli matrices. When ρ_s describes a pure state it is easily seen that the length of the vector $\vec{a}$ must be one. Here we are meeting the important property that to be allowed to treat this vector as a classical one, i.e., to apply the classical equations for its motions, the necessary and sufficient condition is that its length does not change in time. In other words, the length of $\vec{a}$ reflects the correlation between the spin with the radial motion or the entanglement of the spin motion. The case $\vec{a} = 0$ represents an extreme case of quantum correlations. In the following we will also consider the evolution in time of $\mathrm{Tr}(\rho_s^2) = \frac{1}{2}(1 + a^2)$ and the case of full quantum correlations will then be when $\mathrm{Tr}(\rho_s^2) = \frac{1}{2}$.

IV. THE EVOLUTION OPERATOR

The evolution operator of the spin-orbit part alone (1) commutes with the evolution operator of the unperturbed harmonic oscillator. It can be calculated separately. Also we can choose the time unit in order to absorb the constant κ as well as the factor $\frac{1}{2}$ of the spin $\vec{s} = \frac{1}{2}\vec{\sigma}$. In these units $T_{\mathrm{cl}} = \pi/j$. The evolution operator U_s is then written as

$$U_s(t) = e^{it(\vec{l}\cdot\vec{\sigma})} = f(t) + g(t)\,(\vec{l}\cdot\vec{\sigma}) \ . \tag{11}$$

The operators f and g, defined in Eq. (11) are seen to obey the equations

$$i\left(\frac{df}{dt} + \frac{dg}{dt}\,(\vec{l}\cdot\vec{\sigma})\right) = gl^2 + (f - g)(\vec{l}\cdot\vec{\sigma}) \tag{12}$$

or

$$i\frac{df}{dt} = l^2\, g \ , \tag{13a}$$

$$i\frac{dg}{dt} = (f - g) \ . \tag{13b}$$

From now on l^2 is everywhere the square of the orbital angular momentum operator. Equations (13) can be solved formally. The solution corresponding to $f(0) = 1$ and $g(0) = 0$ is

$$f(t) = e^{i\frac{t}{2}}\left[\cos\left(\Omega\frac{t}{2}\right) - \frac{i}{\Omega}\sin\left(\Omega\frac{t}{2}\right)\right] \ , \tag{14a}$$

$$g(t) = e^{i\frac{t}{2}} \left[-\frac{2i}{\Omega} \sin\left(\Omega \frac{t}{2}\right) \right] , \tag{14b}$$

where

$$\Omega = \sqrt{1 + 4l^2} . \tag{15}$$

Note that the factors $1/\Omega$ allow the operators f, and g to be written as infinite series of rational polynomials of l^2.

These expressions for U_s, f, and g are similar to those proposed for the evolution operator of the Jaynes-Cummings model [22]. There this operator was expressed in terms of creation and annihilation operators of photons and acted on coherent states as well as on the states with a fixed number of photons. In our case the states of good orbital angular momentum will be transformed most easily by U_s, while the evolution of coherent states will admix all the partial waves. The similarity to the version of the Jaynes-Cummings model developed in [20] is more transparent if the $\vec{l} \cdot \vec{\sigma}$ operator is expressed in terms of creation and anihilation operators as

$$\begin{aligned} \vec{l} \cdot \vec{\sigma} = i[&(a_z^\dagger a_y - a_y^\dagger a_z)\sigma_x + (a_x^\dagger a_z - a_z^\dagger a_x)\sigma_y \\ &+ (a_y^\dagger a_x - a_x^\dagger a_y)\sigma_z] , \end{aligned} \tag{16}$$

while in [20] the field spin interaction is

$$H_{\text{int}} = a^\dagger a \, (\sigma_+ + \sigma_-) . \tag{17}$$

A. Evolution of a pure $|lm\rangle$ state

Let $|lm\rangle$ be an eigenstate of the operators l^2 and l_z. Since $U_s(t)$ acts only on the angular part of the wave function and on the spin part, the radial part can be left quite arbitrary. Hence $|lm\rangle$ can be any wave packet built in terms of harmonic oscillator wave function with the same l and m.

Because of the simple formula

$$\Omega |lm\rangle = \sqrt{1 + 4l^2} \, |lm\rangle = (2l + 1) \, |lm\rangle , \tag{18}$$

$f(t)$ and $g(t)$ are diagonal and at time t one has

$$U_s(t) \, |lm\rangle = \left[f_l(t) + g_l(t)(\vec{l} \cdot \vec{\sigma}) \right] \, |lm\rangle . \tag{19}$$

In (19) f_l and g_l are simply obtained from (14) by replacing Ω by $(2l+1)$. In order to calculate ρ_s we can use the formulas

$$U_s(t) \, |lm, \pm\rangle = (f_l \pm g_l \, m) \, |lm, \pm\rangle + g_l \, a_\pm(m) \, |lm \pm 1, \mp\rangle \tag{20}$$

with

$$a_\pm(m) = \sqrt{l(l+1) - m(m \pm 1)} , \tag{21}$$

where $|\pm\rangle$ are eigenstates of σ_z with eigenvalues ± 1.

Let us now study the time evolution of the state which has its orbital part in an $|lm\rangle$ state and the spin of which points into the direction $\vec{u} = (\theta, \phi)$ in spherical coordinates:

$$|lm, u\rangle = \cos\left(\frac{\theta}{2}\right) |lm, +\rangle + \sin\left(\frac{\theta}{2}\right) e^{i\phi} \, |lm, -\rangle . \tag{22}$$

A straightforward calculation leads to the matrix elements of ρ_s at time t,

$$\langle + | \rho_s(lm, \theta\phi) | + \rangle$$

$$= \cos^2\left(\frac{\theta}{2}\right) |f_l + g_l \, m|^2 + \sin^2\left(\frac{\theta}{2}\right) |g_l \, a_-(m)|^2 , \tag{23}$$

$$\langle - | \rho_s(lm, \theta\phi) | - \rangle$$

$$= \cos^2\left(\frac{\theta}{2}\right) |g_l \, a_+(m)|^2 + \sin^2\left(\frac{\theta}{2}\right) |f_l - g_l \, m|^2 , \tag{24}$$

$$\begin{aligned} \langle + | \rho_s(lm, \theta\phi) | - \rangle &= \tfrac{1}{2} \sin(\theta) \, e^{i\phi} \, (f_l + g_l \, m)(f_l^* - g_l^* \, m) \\ &= \langle - | \rho_s(lm, \theta\phi) | + \rangle^* . \end{aligned} \tag{25}$$

Because ϕ appears only in the nondiagonal elements as $e^{\pm i\phi}$ the eigenvalues of ρ_s do not depend on ϕ. This result could be expected; since the distribution of the $|lm\rangle$ state has cylindrical symmetry around Oz, there is no reason for the spin part to depend on the angle ϕ. Bohr's frequency $\omega_l = 2l + 1$, which corresponds to the energy separation of the states with $j = l + \frac{1}{2}$ from those with $j = l - \frac{1}{2}$, is the same as the eigenvalue (18) of Ω. The operator $U_s(t)$ has the period $2t_l$, with $t_l = 2\pi/\omega_l$, while ρ_s, which involves the square of $U_s(t)$, has period t_l. More generally, note that

$$U_s(t + t_l) = e^{i\left(\frac{2l+2}{2l+1}\right)} \, U_s(t) . \tag{26}$$

The time t_l of recurrence of a pure state coincides almost with the time $T_{\text{cl}} = \pi/j$ of precession of the classical spin around $\vec{j}$ for large l.

However, there is a considerable change in the nature of the motion of the quantum spin during the interval $(0, t_l)$ compared to the classical motion. Indeed, Eqs. (23)–(25) are far from representing a pure state in the interval $(0, t_l)$. The simplest case to consider is the one where $\theta = 0$ (or $\theta = \pi$ as well). There the density matrix is diagonal and the values of these elements are different from 1 and 0. Since the nondiagonal elements are zero this means that $\langle \sigma_x \rangle = 0$ and $\langle \sigma_y \rangle = 0$. Hence the diagonal elements describe the change in $\langle \sigma_z \rangle$, which is identical in this case to the length of $\vec{a} = \langle \vec{\sigma} \rangle$. The quantum spin vector does not have a constant length and is not settled into a pure state. The evolution during $(0, t_l)$ has nothing to do with a classical rotation: the quantum evolution is the entanglement between the orbital and the spin part. For the case $\theta = 0$ we obtain

$$\langle\sigma_z\rangle = \langle+|\rho_s|+\rangle - \langle-|\rho_s|-\rangle$$
$$= \left[\frac{2m+1}{2l+1}\right]^2 + 4\left[\frac{l(l+1)-m(m+1)}{(2l+1)^2}\right] \times \cos[(2l+1)t] \,. \quad (27)$$

Although Eqs. (4) and (27) are similar mathematically, they correspond to a dynamical phenomenon of quite a different character: the entanglement of the spin with the orbital part takes the place of the classical rotation. The spin is entangled with the $|l\,m\rangle$ and $|l\,m+1\rangle$ states, in the same way as in the Jaynes-Cummings model, to the states $|n\rangle$ and $|n+1\rangle$, where n is the number of photons in the mode. Bohr's frequency $2l+1$ in reduced units takes the place of the Rabi frequency $\sqrt{n+1}$, also in reduced units. Since $\langle\sigma_z\rangle$ is strictly positive for all times, the mixing is never maximal. In the next subsection we will define conditions with coherent states where mixing may be practically maximal.

The general case with $\theta \neq 0$ does not contain any new features except that the density matrix is not diagonal and specific spinors exist that are associated with its eigenvalues. In the general case with $\theta \neq 0$, $\langle\sigma_x\rangle$ and $\langle\sigma_y\rangle$ are generally nonzero.

B. Coherent state

The behavior of the spin discussed above was purely quantum mechanical. Another interesting case can be studied tentatively. We replace the $|lm\rangle$ state by a coherent state of the harmonic oscillator denoted as $|\zeta\rangle$. The aim is to study ρ_s for such a state. Let us write a particular (but general enough for our purpose, as we will see soon) coherent state centered initially at $x = x_0$, $y = 0$, and $z = 0$ and with momentum p_0 along Oy

$$\langle\vec{r}|\zeta\rangle = \pi^{-\frac{3}{4}}\, e^{-\frac{1}{2}\left[(x-x_0)^2+y^2+z^2\right]}\, e^{ip_0 y} \,. \quad (28)$$

This state is specified by two parameters x_0 and p_0 that can be varied in a continuous manner. The numbers ζ_i denote the complex eigenvalues of the annihilation operators $a_i, i = x, y, z$,

$$a_i|\zeta\rangle = \zeta_i|\zeta\rangle \quad (29)$$

with the choice (28) $\zeta_x = x_0/\sqrt{2} = \zeta_x^*$, $\zeta_y = ip_0/\sqrt{2} = -\zeta_y^*$, and $\zeta_z = \zeta_z^* = 0$. Then

$$\langle\zeta|L_z|\zeta\rangle = x_0 p_0 \,, \quad (30)$$

$$\langle\zeta|L_x|\zeta\rangle = \langle\zeta|L_y|\zeta\rangle = 0 \,, \quad (31)$$

and finally

$$\left\langle\zeta\left|\sum_i a_i^\dagger a_i\right|\zeta\right\rangle = |\zeta_x|^2 + |\zeta_y|^2 = \tfrac{1}{2}(x_0^2+p_0^2) \,. \quad (32)$$

Instead of x_0 and p_0 we can characterize our wave packet by the numbers N and L defined as

$$L = x_0 p_0 \,, \quad (33)$$

$$N = \tfrac{1}{2}(x_0^2+p_0^2) \,, \quad (34)$$

where N is the average of the total harmonic oscillator quantum number and L is the average projection of angular momentum of the packet (30) onto the z axis. This allows us to study convenient values of N and L instead of arbitrary values for x_0 and p_0, for example, integer values.

We have calculated the following expectation values in terms of N and L:

$$\langle\zeta|L_z^2|\zeta\rangle = N + L^2 \,, \quad (35)$$

$$\langle\zeta|L^2|\zeta\rangle = 2N + L^2 \,, \quad (36)$$

$$\Delta l^2 = \langle L^2\rangle - \langle L_z\rangle^2 = 2N \,, \quad (37)$$

$$\langle\zeta|L^4|\zeta\rangle = L^4 + 4(N+L^2) + 8N^2 + 8NL^2 \,. \quad (38)$$

The derivation of these equations is straightforward, but somewhat tedious; for example, Eq. (38).

The coherent state (28) contains only two parameters x_0 and $p_{y0} = p_0$ (obviously $p_{x0} = p_{z0} = 0$). These two classical values define one classical orbit oriented in the simplest possible way with its angular momentum along Oz. The evolution operator of the unperturbed harmonic oscillator transforms this state onto a coherent state localized at arbitrary points on this ellipse depending only on the time. Since this operator commutes with U_s, all these points correspond to the same spin density matrix (provided that the spin direction is kept the same with respect to the ellipse). The rotational invariance ensures that it is enough to study the different orientations of the spin with respect to the ellipse. Therefore the spin density matrix depends only on four parameters: two of them refer to the ellipse, such as x_0 and p_0, or equivalently N and L, and the angles θ and ϕ of the spin direction as shown in Fig. 1. The following results are valid for all the central potentials that commute with our special spin-orbit term.

The complete initial state contains the coherent state $|\zeta\rangle$ just defined by (28) times the most general spinor

$$|\zeta, u\rangle = \cos\left(\frac{\theta}{2}\right)|\zeta,+\rangle + \sin\left(\frac{\theta}{2}\right)e^{i\phi}\,|\zeta,-\rangle \,. \quad (39)$$

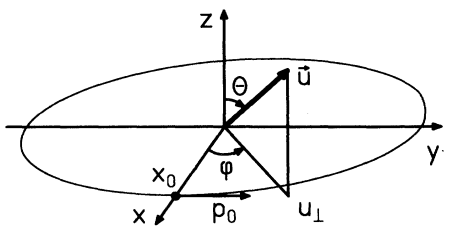

FIG. 1. Picture explaining our convention of variables describing the initial conditions. They are such that the spin points in the direction of $\vec{u}$, while the particle is located at any point on the ellipse; for example, at the point on the minor axis, labeled x_0 with the momentum p_0.

The spin direction is now defined with respect to the axis, which is perpendicular to the elliptic trajectory of the unperturbed wave packet and the minor axis of this ellipse. Our aim now is to discuss the density matrix for the state (39) that is evolved in time by $U_s(t)$, i.e.,

$$|\zeta,u\rangle_t = \left[f(t)+g(t)(\vec{l}\cdot\vec{\sigma})\right] \times\left[\cos\left(\frac{\theta}{2}\right)|\zeta,+\rangle+\sin\left(\frac{\theta}{2}\right)e^{i\phi}|\zeta,-\rangle\right] . \quad (40)$$

1. *Short time limit*

Analytical expressions can be derived for the average values of the spin components along the initial direction $\vec{u}$ as functions of θ, ϕ, N, and L. Since the spin points initially along the $\vec{u}$ direction it is natural to express the density matrix with the matrices σ_u and $\sigma_{u'}, \sigma_{u''}$ ($\vec{u'}$ and $\vec{u''}$ are two directions orthogonal to $\vec{u}$ such that for $\theta = 0$ and $\phi = 0$ one has $\vec{u} = \vec{z}$, $\vec{u'} = \vec{x}$, and $\vec{u''} = \vec{y}$). For small t one finds

$$\langle\sigma_u\rangle_t = 1 + t^2\langle V_s\sigma_u V_s - \tfrac{1}{2}(\sigma_u V_s^2 + V_s^2\sigma_u)\rangle_0 = 1+\alpha_u t^2 , \quad (41)$$

$$\langle\sigma_{u'}\rangle_t = t^2\,\langle V_s\sigma_{u'}V_s - \tfrac{1}{2}(\sigma_{u'}V_s^2 + V_s^2\sigma_{u'})\rangle_0 = \alpha_{u'}\,t^2 , \quad (42)$$

$$\begin{aligned}\langle\sigma_{u''}\rangle_t &= it\langle[V_s,\sigma_{u''}]\rangle_0 \\ &\quad + t^2\,\langle V_s\sigma_{u''}V_s - \tfrac{1}{2}(\sigma_{u''}V_s^2 + V_s^2\sigma_{u''})\rangle_0 \\ &= \beta t + \alpha_{u''}t^2 .\end{aligned} \quad (43)$$

Up to the second order the evolution of the length of the average spin depends only on the following combination of α_u and β^2:

$$a = \left[\langle\sigma_u\rangle_t^2 + \langle\sigma_{u'}\rangle_t^2 + \langle\sigma_{u''}\rangle_t^2\right]^{\frac{1}{2}} \approx 1 + (\alpha_u + \tfrac{1}{2}\beta^2)t^2 , \quad (44)$$

with β defined as

$$\beta = i\langle[V_s,\sigma_{u''}]\rangle_0 = -2\langle l_{u'}\rangle_0 = 2L\sin(\theta) . \quad (45)$$

One finds after some long but simple calculation the coefficient α_u

$$\alpha_u = \langle V_s\sigma_u V_s - V_s^2\rangle_0 = 2\left(\langle l_u\rangle_0 - \langle l_{u'}^2 + l_{u''}^2\rangle_0\right) . \quad (46)$$

In this expression the components $l_u, l_{u'}, l_{u''}$ appear. They can be easily transformed to the fixed axis so that the general result, which is valid for any orbital state, is

$$\begin{aligned}\alpha_u = 2\,\{&\cos(\theta)\langle l_z\rangle_0 - \langle l_x\rangle_0\,[\cos^2(\theta)\,\cos^2(\phi)+\sin^2(\phi)] \\ &-\langle l_y\rangle_0\,[\cos^2(\theta)\,\sin^2(\phi)+\cos^2(\phi)] - \langle l_z\rangle_0\,\sin^2(\theta)\} .\end{aligned} \quad (47)$$

If the initial wave packet possesses the cylindrical symmetry

$$\langle l_x^2\rangle_0 = \langle l_y^2\rangle_0 , \quad (48)$$

the ϕ dependence disappears. This was the case for the $|lm\rangle$ state for which

$$\langle l_x^2\rangle_0 = \langle l_y^2\rangle_0 = \tfrac{1}{2}\left[l(l+1)-m^2\right] . \quad (49)$$

We have proved above that this independence of ϕ survives also for large t for the $|lm\rangle$ state.

In the case of the coherent state (28) we calculate easily the average values of l_x^2, l_y^2, and l_z^2 as

$$\begin{aligned}&\langle l_x^2\rangle_0 = \tfrac{1}{2}p_0^2 \quad , \quad \langle l_y^2\rangle_0 = \tfrac{1}{2}x_0^2 \quad , \\ &\langle l_z^2\rangle_0 = \tfrac{1}{2}(x_0^2+p_0^2) + x_0p_0 .\end{aligned} \quad (50)$$

One can solve Eqs. (33) and (34) in order to express every quantity in terms of N and L. Our choice for x_0 and p_0 is such that

$$x_0^2 = N - \sqrt{N^2-L^2} \quad , \quad p_0^2 = N + \sqrt{N^2-L^2} . \quad (51)$$

The coefficient of interest in Eq. (44) can now be expressed as

$$\begin{aligned}\gamma_u = \alpha_u + \tfrac{1}{2}\beta^2 = 2\,\{&L\,\cos(\theta) - N[1+\tfrac{1}{2}\sin^2(\theta)] \\ &+\tfrac{1}{2}\sqrt{N^2-L^2}\,\cos 2(\phi)\,\sin^2(\theta)\} .\end{aligned} \quad (52)$$

The eigenvalues of the density matrix up to t^2 are simply

$$1+\tfrac{1}{2}\gamma_u t^2, \quad -\tfrac{1}{2}\gamma_u t^2 . \quad (53)$$

It is obvious that our result must have a period π with respect to ϕ. The dependence on ϕ disappears for $N = L$ since the trajectory is circular. We also find in this case that the circle is indeed oriented with respect to spin since $\gamma_u = 0$ if $\theta = 0$, while $\gamma_u = -4L$ for $\theta = \pi$. Finally, in the interesting case $L = 0$, γ_u takes the form

$$\gamma_u = -2N\left[1+\cos^2(\psi)\right] , \quad (54)$$

where ψ is the angle between u, the spin direction, and the long axis (Ox) of the ellipse. Indeed, for $L = 0$, only one angle, the angle ψ, appears since the trajectory is linear.

The conclusion for the short time limit is similar to that drawn for the $|lm\rangle$ state. The coherent state (39) behaves immediately when $t = 0+\epsilon$ in such a way that the spin part and the orbital part are entangled. Moreover, there is no hope to change this behavior by increasing N and L, i.e., in the case where the coherent state is supposed to behave even more classically.

2. *Long time behavior*

The next task is to follow the spin evolution for larger t. We have chosen to decompose the coherent state $|\zeta\rangle$ on the spherical harmonic oscillator basis $|nlm\rangle$ using an old work by Mikhailov [19]. Let us write

$$|\zeta\rangle = \sum_{nlm} \lambda_{nlm}(\zeta)\,|nlm\rangle\ . \tag{55}$$

Mikhailov has shown that

$$\lambda_{nlm}(\zeta) = e^{-\frac{N}{2}} \sqrt{\frac{(2l+1)!!\,2^j}{j!\,(l+n+1)!!}}\ (\zeta_+\zeta_- - \tfrac{1}{2}\zeta_0^2)^j \times \sqrt{\frac{l!\,(l+m)!\,(l-m)!}{(2l)!}} \times \sum_{\rho} \frac{(\zeta_+)^{(l+m-\rho)/2}\,(\sqrt{2}\zeta_0)^{\rho}\,(\zeta_-)^{(l-m-\rho)/2}}{\left(\frac{l+m-\rho}{2}\right)!\,\rho!\,\left(\frac{l-m-\rho}{2}\right)!}\ , \tag{56}$$

where $j = \frac{1}{2}(n-l)$ and $\rho = 1,3,5,\ldots$ for $l+m$ odd and $\rho = 0,2,4,\ldots$ for $l+m$ even, while $\zeta_\pm = \mp 1/\sqrt{2}(\zeta_x \mp i\zeta_y)$ and $\zeta_0 = \zeta_z$ (zero in our case). The expansion of a coherent state in partial waves has recently been studied by Boris *et al.* [23] in the framework of their study of Kepler orbits of H atoms. Our formulas (35)–(37) show that indeed there is a spread in angular momentum given by $\Delta L/\langle L_z\rangle = \sqrt{2N}/L$, which decreases with L, while there is also a spread in the number N, which is given by $\Delta N/N = 1/\sqrt{N}$ and decreases with N. The time evolution is obtained by writing the wave packet in the form

$$|\zeta,\vec{u}\rangle = \sum_{nlm} \lambda_{nlm}(\zeta)\,|nlm\rangle \left[\cos\left(\frac{\theta}{2}\right)|+\rangle + \sin\left(\frac{\theta}{2}\right) e^{i\phi}|-\rangle\right]\ . \tag{57}$$

The evolution in time is obtained by using Eq. (20) on each term of this sum. Obviously, the density matrix is a sum of terms corresponding to all the values of n and l which are present in (57); the density matrix is shown in the Appendix. Because of Eq. (20) each factor has period $2\pi/(2l+1)$ and the sum admits the common period 2π, which is also a multiple of the classical period π/j. Note, however, that the admixture of many partial waves does not improve the connection between the quantum period and the classical one. The quantum period resembles the classical period for a pure $|lm\rangle$ state for large l. We have discussed the large difference in the nature of the dynamics of the two cases. The admixture of many partial waves produces only a multiple of the period.

Another difference with respect to the case of the pure $|lm\rangle$ state stems from the ϕ dependence of the density matrix. Indeed, one can easily see that the angle ϕ, when the sum of (57) involves different values of m, occurs also in the diagonal elements of ρ_s. This confirms our previous result of Eq. (47) that the eigenvalues of the density matrix depend now on ϕ. The calculations of the density matrix and its diagonalizations have been performed numerically.

V. NUMERICAL RESULTS FOR SPIN $\frac{1}{2}$

We will now present the behavior of two quantities $\mathrm{Tr}(\rho_s^2) = \frac{1}{2}(1+a^2)$ and $\langle\sigma_u\rangle = \mathrm{Tr}(\rho_s\sigma_u)$ as functions of t/T. Here T is the common period of all partial waves corresponding to a fixed value of the coupling constant κ; it takes the value $T = 2\pi$ and appears in all the quantities that were calculated. The period of the harmonic oscillator is absent from all our results because it cancels in the calculation of ρ_s. Pure spin states are recurrent for multiple times of T. The time reversal symmetry combined with the T periodicity allows us to understand why all quantities are symmetric with respect to the time $\frac{1}{2}T$. The evolution operator U_s is indeed such that

$$U_s(-t) = U_s^*(t)\ . \tag{58}$$

From Eq. (26) one also gets

$$U_s(t+T) = U_s(t)\ . \tag{59}$$

Combining all these properties, one obtains

$$\rho_s(t) = \rho_s(-t) = \rho_s(-t+T)\ , \tag{60}$$

$$\rho_s(\tfrac{1}{2}T - t) = \rho_s(\tfrac{1}{2}T + t)\ . \tag{61}$$

We have concentrated our efforts on two values of the principal quantum numbers that were chosen as integers: $N = 8$ and $N = 20$. They are supposed to correspond to a low value and a higher value of the excitation energy, respectively. In each case L was varied by integral steps from 0 to N, while θ and ϕ were given simple values.

In Figs. 2 and 3 we present $\mathrm{Tr}(\rho_s^2)$ and $\langle S_u\rangle$ as functions of t/T. The curves correspond to $\phi = 0$, i.e., when $\theta = \frac{1}{2}\pi$ the spin points along the short axis of the elliptic trajectory. The curves for $N = 8$ and $N = 20$ are qualitatively similar as far as the behavior with respect to t, L, and θ is concerned.

The general behavior can be described in the following terms. There is a rapid decrease of $\mathrm{Tr}(\rho_s^2)$ for very small t. Let us call this time the "collapse time," which can be defined using our Eq. (53) as

$$\tau_c = \frac{1}{\sqrt{|\gamma_u|}}\ . \tag{62}$$

This behavior very much resembles what is observed in the Jaynes-Cummings model (Fig. 1 of the first work of [14]; see also [22]). There the spin state, a pure state for $t = 0$, collapses to a maximum mixing since $\mathrm{Tr}(\rho_s^2) = \frac{1}{2}$. In our case the character of the mixing that is obtained depends very much on θ and L. The value $\theta = \frac{1}{2}\pi$ leads to the largest change. For $L = N$ a value very near from $\frac{1}{2}$ is indeed obtained for $\theta = \frac{1}{2}\pi$, but for $L = 0$, 2, or 4 the mixing is incomplete. The collapse time is much shorter for $N = 20$ than for $N = 8$, as predicted by (52). Note that as long as $\mathrm{Tr}(\rho_s^2) = \frac{1}{2}$, then $|\langle\vec{\sigma}_u\rangle| = 0$.

The collapse time corresponds to the time needed for the partial waves of the wave packet to get out of phase. A partial revival is possible for $t/T = \frac{1}{2}$, as shown in Figs. 2 and 3, which also during a time τ_c and is quite

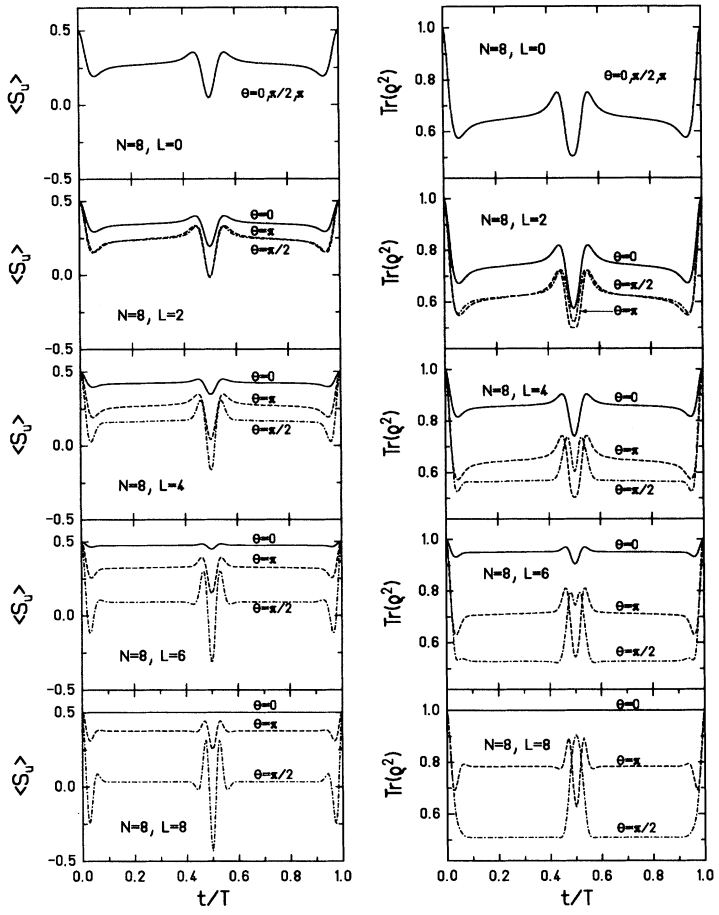

FIG. 2. Expectation value of the spin component and the trace of ρ_s^2 as functions of time during one period for three different initial positions of spin vector with respect to the orbit. For all cases $\phi = 0$ and $N = 8$ (low excitation energy).

spectacular for $\theta = \frac{1}{2}\pi$ and $L = N$. In this case the revival is characterized by $\mathrm{Tr}(\rho_s^2) \approx 1$ and

$$\langle \sigma_u \rangle_{T/2} \approx -\langle \sigma_u \rangle_0 \ . \tag{63}$$

The case $L = N$ enables us to understand almost analytically those behaviors. In this case the sum (55) is restricted to $m = l$ and $l = n$,

$$|\zeta\rangle = \sum_l \lambda_{lll}(\zeta)|lll\rangle \ . \tag{64}$$

The matrix ρ_s is then obtained by using Eqs. (23)–(25) for all the partial waves with $m = l$. One finds

$$\langle +|\rho_s|+\rangle = \cos^2\left(\frac{\theta}{2}\right) + \sin^2\left(\frac{\theta}{2}\right) a(t) \ , \tag{65}$$

$$\langle -|\rho_s|-\rangle = \sin^2\left(\frac{\theta}{2}\right) b(t) \ , \tag{66}$$

$$\langle +|\rho_s|-\rangle = \tfrac{1}{2}\sin(\theta)\ e^{-i\phi}\, c(t) \ , \tag{67}$$

with the coefficients $a(t)$, $b(t)$, and $c(t)$ defined as

$$a(t) = \sum_l \Lambda_l \frac{8l}{(2l+1)^2} \sin^2\left(\frac{2l+1}{2}t\right) \ , \tag{68}$$

$$b(t) = \sum_l \Lambda_l \left[\cos^2\left(\frac{2l+1}{2}t\right) + \left(\frac{2l-1}{2l+1}\right)^2 \sin^2\left(\frac{2l+1}{2}t\right)\right] \ , \tag{69}$$

$$c(t) = \sum_l \Lambda_l\ e^{-i\frac{2l+1}{2}t}\left[\cos\left(\frac{2l+1}{2}t\right) - i\frac{2l-1}{2l+1}\sin\left(\frac{2l+1}{2}t\right)\right] \ . \tag{70}$$

For the simple case studied with $L = N$, Eq. (56) leads to the simple result

$$\Lambda_l = |\lambda_{lll}|^2 = e^{-N}\frac{N^l}{l!} \ , \tag{71}$$

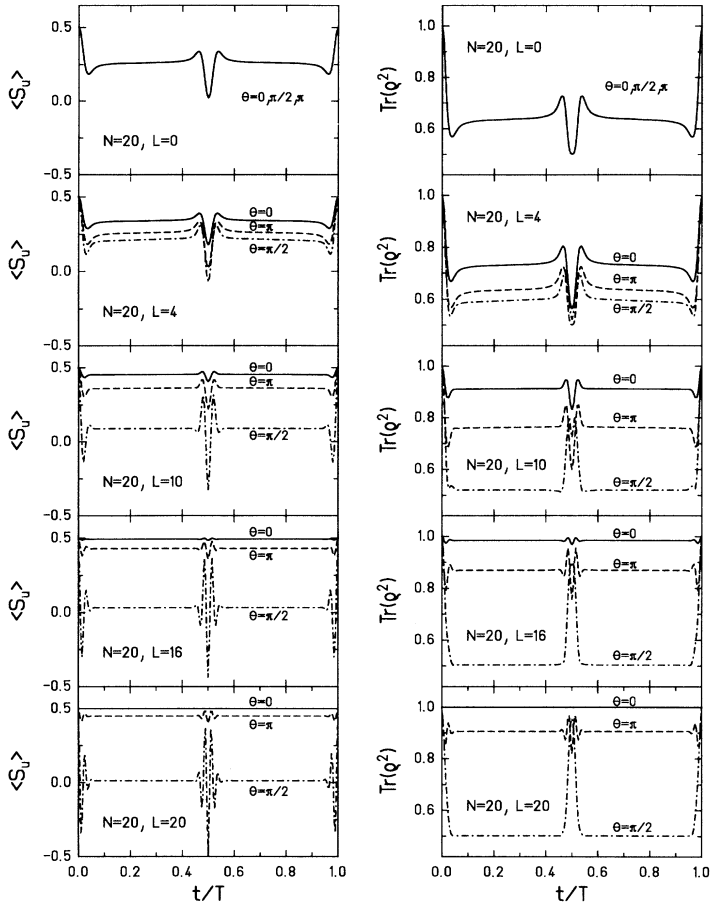

FIG. 3. Same as in Fig. 2, but for $N = 20$ (high excitation energy).

exactly the Poisson distribution. (Note that $\sum_l \Lambda_l = 1$.) However, the detailed form of Λ_l is somewhat irrelevant in the following discussion.

From this matrix the following behaviors for $L = N$ are seen.

(i) For $\theta = 0$ the eigenvalues are 0 and 1 for any t.

(ii) The eigenvalues of ρ_s are independent of ϕ. (The density distribution is indeed circular.)

(iii) For $\theta = \pi$ the eigenvalues of ρ_s are $a(t)$ and $b(t)$. For high N the high l play a dominant role, as seen in [22], and therefore

$$a(t) \approx 0, \qquad b(t) \approx 1\ . \tag{72}$$

For $N = 20$ the numerical calculation shows that indeed $\mathrm{Tr}(\rho_s^2) \approx 0.9$ and we are not far from the high l limit.

(iv) For $\theta = \frac{1}{2}\pi$ the element $\langle +|\rho_s|-\rangle$ is different from zero, but Eq. (70) shows that all the phases are present for a general t. Therefore, on the average, the density matrix is $\frac{1}{2}$ in the diagonal and 0 elsewhere. This is the case of maximum mixing.

(v) For $\theta = \frac{1}{2}\pi$ and $t/T = \frac{1}{2}$ the coefficient $c(\pi)$ takes a finite value and the partial waves add coherently

$$c(\pi) = -\sum_l \Lambda_l \left(\frac{2l-1}{2l+1}\right)\ . \tag{73}$$

Using the same approximation as above for the high N, $c(\pi) \approx -1$. The density matrix is now

$$\rho_s(\pi) = \begin{vmatrix} \frac{1}{2} & -\frac{1}{2}e^{-i\phi} \\ -\frac{1}{2}e^{i\phi} & \frac{1}{2} \end{vmatrix}\ . \tag{74}$$

It describes also a pure state. Since initially

$$\rho_s(0) = \begin{vmatrix} \frac{1}{2} & \frac{1}{2}e^{-i\phi} \\ \frac{1}{2}e^{i\phi} & \frac{1}{2} \end{vmatrix}\ , \tag{75}$$

the spin is found rotated by π in the plane xOy after this time $\frac{1}{2}T$. The numerical calculation corresponds quite well for $N = 20$ to the limit just described. The secondary maximum or minimum that occurs near $t = 0$ or $t = \frac{1}{2}T$ is not understood. They could be connected to some partial revivals, but their amplitudes are very small.

Our numerical calculation shows that the explanations given for $L = N$ apply also to the behavior of ρ_s for $L < N$. This confirms that our collapse time is generally the time of dephasing of the partial waves. We can note, however, that $\mathrm{Tr}(\rho_s^2)$ is minimum for $\theta = \frac{1}{2}\pi$ and for $t = \frac{1}{2}T$ there is not always a revival in general. The revival occurs near $L = N$ and $L = 0$ in both cases; it corresponds to a reversal of the spin with respect to its initial value.

The general case is, however, more difficult to interpret since not only the values $m = l$ contribute to the expansion (55). Therefore, ρ_s takes a more complex form and the analysis is more difficult.

Generally, our results depend on θ and ϕ. For $L = 0$, as said above, the relevant angle is the angle ψ defined for Eq. (54). This explains why the curves $\theta = 0$, $\frac{1}{2}\pi$, and π coincide in Figs. 2 and 3 when $L = 0$. For $L \neq 0$ the curves with different θ are split. A maximum difference occurs for $L = N$ between $\theta = 0$ and $\theta = \frac{1}{2}\pi$. Moreover, it is for these values of L that the revival appears when $\theta = \frac{1}{2}\pi$. It is interesting to follow the revival as a function of ϕ and L. As we have represented in Fig. 4, the revival occurs even for $L = 0$ when $\psi = \frac{1}{2}\pi$, i.e., when spin is directed initially along the long axis. A similar conclusion is also drawn from Fig. 5, where we have studied the occurrence of the revival when the spin points initially in the plane xOy for $L = 4 = \frac{1}{2}N$. The revival is observed for $\phi = \frac{1}{2}\pi$. It has the same property: the spin state is almost pure for $t = \frac{1}{2}T$ and the spin is reversed.

Finally, the values of $\langle \sigma_u \rangle$ and $\mathrm{Tr}(\rho_s^2)$ at $t = \frac{1}{2}T$ are given as a function of L for $N = 20$ in Table I. It is seen that the revival is a general phenomenon which is present for all values of L and N provided that the spin is well located initially, i.e., toward the long axis of the ellipse. A maximum value of $\mathrm{Tr}(\rho_s^2)$ is observed in Table I for $L = \frac{1}{2}N$.

It is interesting to compare the evolution of the density matrix and of the spin in the vicinity of $t = 0$ and $t = \frac{1}{2}T$. In Fig. 6 the curves for $t \approx 0$ and $t \approx \frac{1}{2}T$ have been superposed. We have chosen $N = 20$, $L = 10$, and of course $\vec{s}$ pointing initially toward the long axis. The spin evolution around these two values of time is very similar. We have obtained similar results for other values of L. Therefore, there is a common dynamics of collapse and revival that is characterized by the coefficient γ_u, which we have calculated analytically.

When the purity of the spin state is brought back,

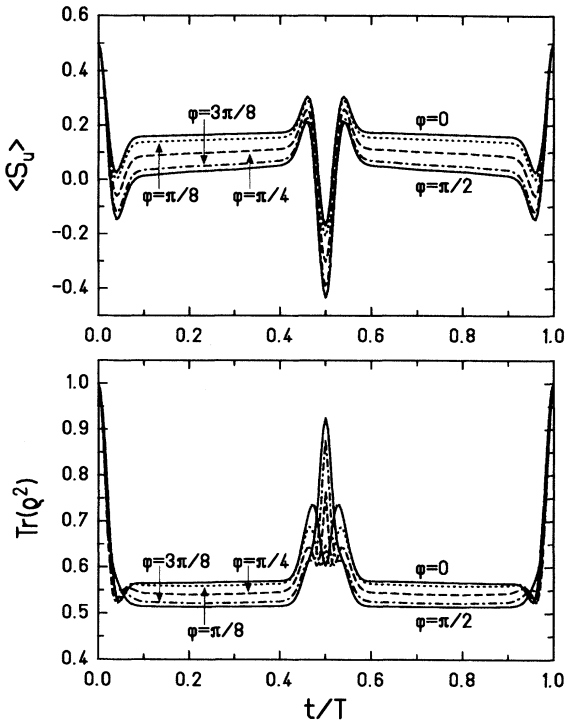

FIG. 5. Illustration of the dependence of $\langle S_u \rangle$ and $\mathrm{Tr}(\rho_s^2)$ on the ϕ angle for $N = 8$ and $L = 4$. Note that in this case $\theta = \frac{1}{2}\pi$.

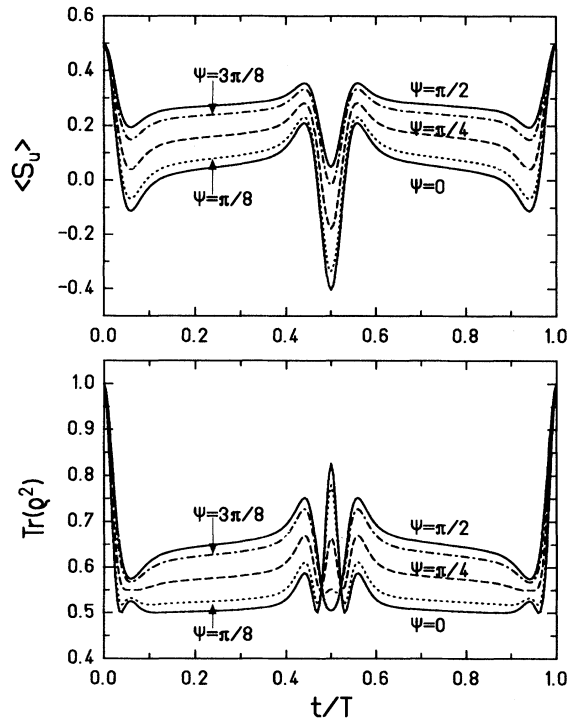

FIG. 4. Time evolution of the system with linear classical trajectory for $N = 8$ and $L = 0$. The different initial positions of spin with respect to the trajectory are given by the ψ angle.

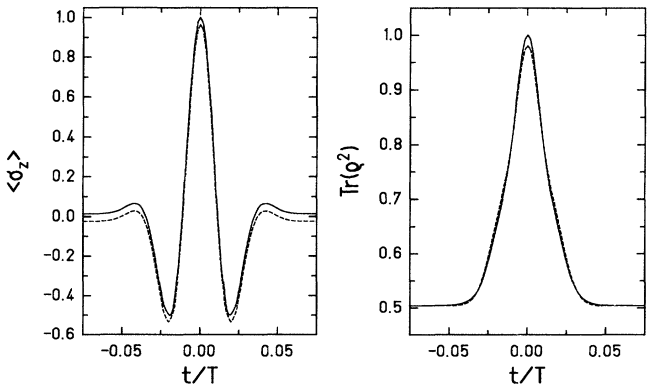

FIG. 6. The detailed study of the exact revival at $t = nT$ (solid line) with the approximate one at $t = (n + \frac{1}{2})T$, obtained with particular initial conditions $\theta = \phi = \frac{1}{2}\pi$ (dashed line) for $N = 20$ and $L = 10$. The latter case has been superposed on the former one (shifted by 0.5 along horizontal axis) for better comparison.

TABLE I. The degree of the revival at $t = \frac{1}{2}T$ for wave packets with $N = 20$.

L	$\langle\sigma_u\rangle$	$\mathrm{Tr}(\rho_s^2)$
0	-0.911694	0.915592
2	-0.916264	0.924034
4	-0.928176	0.943642
6	-0.943576	0.963163
8	-0.954722	0.975467
10	-0.962580	0.980189
12	-0.966378	0.980145
14	-0.967334	0.977938
16	-0.966386	0.974732
18	-0.963428	0.970256
20	-0.948642	0.954952

the spatial state is also in a pure state. It is not hard to see that the spatial state revives to a coherent state centered on the classical ellipse at the place where the classical particle would be found without spin-orbit coupling. For $t = nT$ the revival of the coherent state is complete, but for $t = (n + \frac{1}{2})T$ we can expect it only approximately. However, the details of the time evolution of spatial degrees of freedom require the analysis of the complementary reduced density matrix ρ_r.

It is interesting to analyze the consequences of the changes of $\langle\vec{\sigma}\rangle$ on the average of the orbital angular momentum. Let us note that on the average $\langle\vec{j}\rangle = \langle\vec{l} + \vec{s}\rangle$ is conserved. To be more specific, let us consider the case $L = N$ and $\theta = \frac{1}{2}\pi$ in which we have a sharp transition to $\mathrm{Tr}(\rho_s^2) \approx \frac{1}{2}$. Initially the only nonzero component of $\langle\vec{l}\rangle_0$ is $\langle l_z\rangle_0 = L$, while that of $\langle\vec{s}\rangle_0$ is $\langle s_x\rangle_0 = s$. In the mixed state with $\langle\vec{s}\rangle_t \approx 0$, the average value of the orbital angular momentum must be such that $\langle l_x\rangle_t \approx s$, and $\langle l_z\rangle_t \approx L$ during all the time when $\mathrm{Tr}(\rho_s^2) \approx \frac{1}{2}$. When $\frac{t}{T} = \frac{1}{2}$, thus $\langle\vec{l}\rangle_{T/2}$ should take an other value since $\langle s_x\rangle_{T/2} \approx -s$. The conservation of $\langle\vec{j}\rangle$ provide the values $\langle l_x\rangle_{T/2} \approx 2s$ and $\langle l_z\rangle_{T/2} \approx L$. We obtain a situation where the amount of angular momentum transported by the spin is carried out by the orbital part of the wave function in such a way that the length and the direction of the vector $\langle\vec{l}\rangle$ are changed [24]. This change is an increase of $\langle l_x\rangle$ from 0 to $2s$ made in two steps. The first occurs during the interval $[0, \tau_c]$, where $\langle l_x\rangle$ increases by s; the second one occurs during the interval $[\frac{T}{2} - \tau_c, \frac{T}{2}]$. The reverse changes of $\langle l_x\rangle$ are produced in the second interval $[\frac{T}{2}, T]$.

All the changes of $\mathrm{Tr}(\rho_s^2)$ in which the length of $\langle\vec{s}\rangle$ decreases can be described by a modification of $\langle\vec{l}\rangle$ which gains or loses the corresponding amount of angular momentum. Figures 2 and 3 show that we have to consider extreme situations when $\theta = \frac{1}{2}\pi$ and a large N and L to be able to produce the maximum transition between $\langle\vec{s}\rangle$ and $\langle\vec{l}\rangle$ that we have described above.

VI. CASE OF HIGHER SPIN

Along the same lines as Ballentine [12] we want to investigate also the limit of a higher spin. We consider from now that there are $2S+1$ spin states with $S > \frac{1}{2}$. In order to produce a spread of spin-orbit multiplets independent of S, the spin-orbit interaction (1) will be replaced by

$$V_S = \frac{\kappa}{S}(\vec{l}\cdot\vec{S}) \,. \tag{76}$$

(The change of S can also be incorporated in the time scale by eventually replacing t by St.)

Here we benefit from the discussion about $S = \frac{1}{2}$. We have learned that the most rapid change of ρ_s occurs initially and therefore we want to estimate how the collapse time depends on S. We keep again the spin along $\vec{u}$ at time 0 and consider, as at the beginning of the Sec. IV B 1 a general wave packet. Along the same lines as for Eq. (41)–(44), one finds, for the average value of the spin length at time t,

$$\begin{aligned}|\langle\vec{S}\rangle|_t &\approx \langle S_u\rangle_0 + t^2\,[\langle V_S S_u V_S - \tfrac{1}{2}(S_u V_S^2 + V_S^2 S_u)\rangle_0 \\ &\quad + \tfrac{1}{2S}|\langle[V_S, S_{u''}]\rangle_0|^2] \qquad (77)\\ &= S + t^2\Big[\langle V_S S_u V_S\rangle_0 - S\langle V_S^2\rangle_0 \\ &\quad + \tfrac{1}{2S}|\tfrac{i}{S}\langle S_u l_{u'}\rangle_0|^2\Big] \qquad (78)\\ &= S + \frac{t^2}{2S^2}\{\langle l_u\rangle_0\,[S(S+1) - S^2] \\ &\quad - \langle l_{u'}^2 + l_{u''}^2\rangle_0\, S + S\langle l_{u'}\rangle_0^2\} \,. \qquad (79)\end{aligned}$$

In the case $S = \frac{1}{2}$ the coefficient of t^2 in (79) is $\frac{1}{2}$ times the coefficient γ_u, which is given in (46) because $\vec{S}$ is used instead of $\vec{\sigma}$. After the transformation to the fixed axis as in Eq. (47), the following equation is obtained for the coherent state, again using (50):

$$\begin{aligned}|\langle\vec{S}\rangle|_t &\approx S + \frac{t^2}{2S}\{L\cos(\theta) - N[1 + \tfrac{1}{2}\sin^2(\theta)] \\ &\quad + \tfrac{1}{2}\sqrt{N^2 - L^2}\cos 2(\phi)\,\sin^2(\theta)\} \qquad (80)\\ &= S + \frac{\gamma_u}{4S}\,t^2 \,. \qquad (81)\end{aligned}$$

This simple formula shows that S occurs only in the denominator or, more simply, that the collapse time of the spin scale as $\sqrt{S}$ since, concerning the N, L, θ, and ϕ dependence, the coefficient γ_u is the same for general S as for $S = \frac{1}{2}$ (52) for small t. The expectation value (80) just calculated does not coincide, however, for $S \neq \frac{1}{2}$ with the time evolution of $\mathrm{Tr}(\rho_s^2)$ as it does for $S = \frac{1}{2}$ since the density matrix is characterized now not only by the vector $\langle\vec{S}\rangle$, but by an increasing number of tensors of higher rank that we cannot calculate easily. Therefore, the numerical calculation of $\mathrm{Tr}(\rho_s^2)$ is an interesting task.

We have plotted in Fig. 7 $\langle S_z\rangle$ and $\mathrm{Tr}(\rho_s^2)$ for $N = 8, L = 4$, and $S = \frac{1}{2}, \frac{5}{2}, \frac{9}{2}, \frac{13}{2}$ as functions of t for two different initial conditions: the spin parallel (left) and perpendicular (along the long axis of the ellipse—right) to the angular momentum. For a better comparison $\langle S_z\rangle$ is scaled with respect to S. As for higher S time units scale with S ($T_S = S\,T_{\frac{1}{2}}$); the small t behavior is clearly

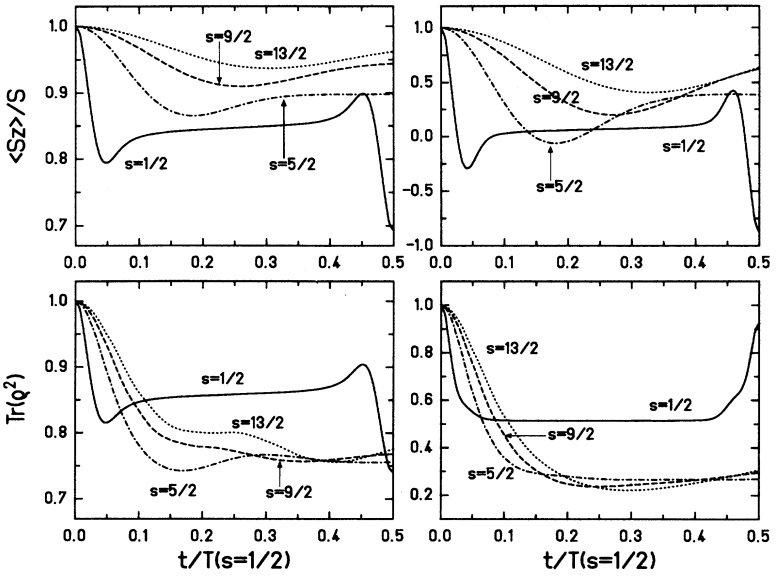

FIG. 7. Short time behavior of the relevant quantities for different S values and $N = 8$ and $L = 4$. All time units are that of the system with $S = \frac{1}{2}$. The left part corresponds to the case when spin and angular momentum are initially parallel ($\theta = 0$), the right one when they are perpendicular ($\theta = \varphi = \pi/2$).

seen. Indeed the behavior obtained in (81) is observed. However, the mixing regime dominates for a longer time for all $S = \frac{5}{2}, \frac{9}{2}, \frac{13}{2}$ and there is no indication of a decrease with S.

In Fig. 8 we display the full time dependence (having in mind the symmetry with respect to $t = \frac{1}{2}T$ [Eq. (61)]) of $\langle S_z \rangle$ (divided by S) and $\mathrm{Tr}(\rho_s^2)$ for $N = 8, L = 4$, and $S = \frac{9}{2}$. The four curves correspond to the initial spin positions parallel, antiparallel, and perpendicular (in this case either along the long or the short axis of the ellipse) with respect to the angular momentum. The upper part looks similar to the $S = \frac{1}{2}$ case; the behavior is smooth, and only the curve corresponding to $\theta = \phi = \pi$ exhibits a richer structure. Concluding from only $\langle S_z(t) \rangle$ is, however, misleading because the lower part shows a much richer time dependence. In particular, a peak occurs for $t/T = \frac{1}{4}$, which is not explained. But the general behavior is the same as for $S = \frac{1}{2}$: the spin spends most of the time in a highly mixed state and there is no clear approach of a classical regime.

After diagonalization of spin density matrix ρ_s one can calculate another quantity describing the mixed system—entropy:

$$S(\rho_s) = -\mathrm{Tr}\, \rho_s \ln \rho_s \,. \tag{82}$$

We do not present it because $S(\rho_s)$ contains exactly the same information as $\mathrm{Tr}(\rho_s^2)$.

VII. A POSSIBLE EXTENSION TO THE HYDROGEN ATOM

We will now propose an extension of our results to wave packets in the hydrogen atom taking into account the spin-orbit interaction. Let H_0 now be the central part of the Hamiltonian, while spin-orbit part (1) is replaced by

$$V_s = \frac{1}{2} R\alpha^2 \left(\frac{a_0}{r}\right)^3 (\vec{l} \cdot \vec{s}) \,, \tag{83}$$

where R, α, and a_0 are, respectively, the Rydberg constant, the fine structure constant, and the Bohr radius.

It is a difficult task to provide closed formulas for $\rho_s(t)$ for a general wave packet in the H-atom case. We will limit ourselves to the case considered in Appendix B, where all the partial waves appear in the expansion with

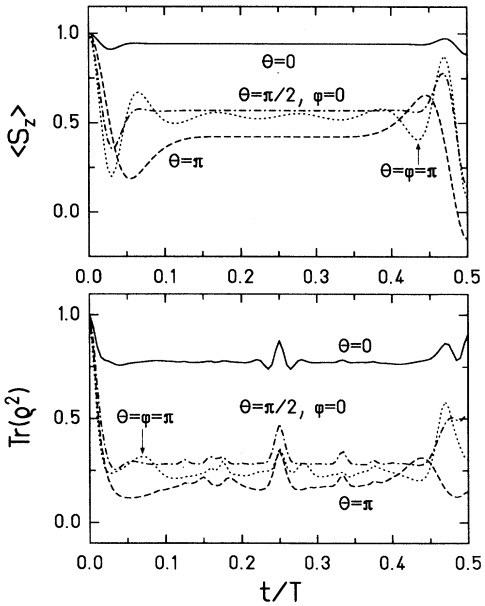

FIG. 8. An example of time evolution of $S = \frac{9}{2}$ system for several initial conditions (indicated in the picture) and for $N = 8$ and $L = 4$. The time range is limited to only half of the period to show more precisely the details [the second half of the period is a mirror reflection of the first one due to symmetries (58)–(61)].

$m = l$ only and a single radial quantum number n_l also occurs. We will choose $n_l = l + 1$, with the usual spectroscopic notation. On the other hand, the partial waves will be distributed in such a way that, like in Eq. (71),

$$|\lambda_{n_l l l}|^2 = e^{-N} \frac{N^l}{l!} , \tag{84}$$

Our initial wave packet is then characterized by some integer N and by an initial average angular momentum L such that $L = N$. We have proved in Eq. (B4) that $\rho_s(t)$ depends only on V_s defined by (83). The difference with the case of the harmonic oscillator considered previously is that V_s contains a function of r, $V_0(r) = \frac{1}{2}R\alpha^2(\frac{a_0}{r})^3$, which can be treated by first-order perturbation theory. The radial integrals for the states with $n_l = l + 1$ are expressed as [25]

$$\left\langle n_l = l+1\, l \left| \frac{1}{r^3} \right| n_l = l+1\, l \right\rangle = \frac{1}{a_0^3\, l(l+1)^4(l+\frac{1}{2})} . \tag{85}$$

These integrals produce a splitting between the spin-orbit partners with $n_l = l + 1$, $j = l + \frac{1}{2}$, and $j = l - \frac{1}{2}$ given by (in units $\frac{1}{2}R\alpha^2$)

$$\omega_l = \frac{2}{l(l+1)^4} . \tag{86}$$

There is a strong decrease of ω_l with l that shows that only a few partial waves contribute. Treating V_0 by first-order perturbation theory allows us to use Eqs. (65)–(67) for the matrix elements of $\rho_s(t)$ with $a(t)$, $b(t)$, and $c(t)$ defined as in Eqs. (68)–(70), but with the frequency $2l+1$ in the time functions replaced by that defined by Eq. (86). Obviously the time unit is different from that in the harmonic oscillator. We can choose this unit in such a way that $T_{l=1} = 1$.

A justification of our decoupling of the spin motion from the orbital motion can be found when considering those classical orbits which are such that the electron stays on a sphere. Such orbits are indeed possible and provide simple classical analog to our wave packet.

The results presented in Fig. 9 for $N = L = 4$ and $\theta = \frac{1}{2}\pi$ show that only a few partial waves occur. The significant change of $\mathrm{Tr}(\rho_s^2)$ observed is explained by the three highest frequencies with $l = 1$, 2, and 3. The interference of these three waves produces a value $\mathrm{Tr}(\rho_s^2) \approx 0.55$ after about three periods of $l = 3$ wave. However, we do not get a collapsed state stable in time and the oscillatory character takes over. The highest frequency, due to $l = 1$, is presented in the inset of Fig. 9 for a small time interval and enlarged vertical scale. This frequency is not seen on the long time behavior where the fastest oscillations are due to the wave with $l = 2$, while the oscillations with a longer period which mimic the revivals are due to the wave with $l = 3$. (Note that for $N = 4$ the Poisson distribution is maximum for this partial wave.)

In conclusion, this model shows, besides the change of scale already explained, an evolution for the H atom in which only a few spin-orbit partners are involved. This evolution is devoid of a reasonable revival; it presents a situation where the state is neither totally pure nor totally mixed.

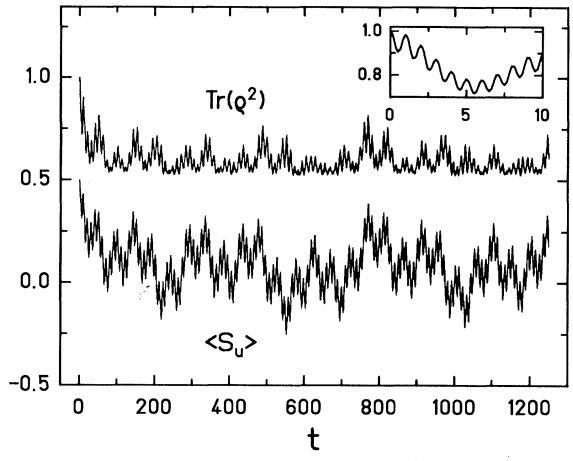

FIG. 9. The time evolution of $\mathrm{Tr}(\rho_s^2)$ and $\langle S_u \rangle$ for the circular trajectory of the spatial wave packet in the hydrogen atom with $N = L = 4$ and $\theta = \pi/2$. The period of the partial wave with $l = 1$ (the highest frequency contribution) is chosen as the time unit. The initial position of spin is perpendicular to the trajectory in its plane. The inset shows the presence of the highest frequency in the $\mathrm{Tr}(\rho_s^2)$ curve for short times. In the full picture this highest frequency is residually seen only in the thickening of both curves.

VIII. CONCLUSION

The aim of this paper was to underline the difference between the quantum evolution of the spin and the classical one in cases where there is a spin-orbit potential added to a central one. For $S = \frac{1}{2}$ we have found no way for a transition toward a classical behavior. Quantum mechanics describes the spin evolution as its entanglement with the orbital part, which cannot be suppressed by an increase of the quantum numbers of the spatial wave packet. This entanglement has been studied as a function of the initial conditions; it can be totally suppressed only in some trivial cases when $\vec{s}$ and $\vec{l}$ are totally decoupled. It is a common feature of the spin-orbit model and of the Jaynes-Cummings model that there is a collapse of the spin state that occurs as soon as the coupling is effective. It is a second common feature that the entanglement does not last forever and that there are revivals. We have found an interesting case where the revival is produced when the spin is found pointing in a direction that is opposite the initial one. The quantum-mechanical period that is found in the spin-orbit problem for the case of a coherent state depends only on the strength κ of the spin-orbit interaction. Thus it is independent of the initial conditions and in particular of the orbital angular momentum or of the total angular momentum. In a sim-

ilar configuration the classical period depends on κ as well as on j through formula (3).

It is worth mentioning the existence of a different semiclassical approach to spin–orbit coupling developed by Littlejohn and Flynn [26] and Frisk and Guhr [27], whose aim is to treat spin degrees of freedom exactly. However, they concentrate their considerations on a spatial part; a possible connection of the entanglement of the spin with spatial degrees of freedom with results obtained within their approach is not clear for us.

When the spin-orbit interaction acts between a number $2S+1$ of spin-orbit partners, a collapse is also produced, but there is only a slow increase of the collapse time like $\sqrt{S}$. None of our numerical calculations produce a result closer to the classical result.

We have also considered spin-orbit splittings with a law identical to that presented in the H atom. There is certainly a tendency toward mixing. However, the behavior of the density matrix is explained there only by a few frequencies, while the different partial waves produce a collective collapse for the harmonic oscillator. This certainly permits us to ignore the spin evolution in the hydrogen atom for the time scale considered until now [2,3,22].

We have shown in this paper that the spin-orbit problem in a spherical harmonic oscillator presents a striking similarity to the problem of a two-level system interacting with a one-mode field in a cavity. Both of these models emphasize the original way in which a spin is coupled to its quantum-environment in quantum mechanics.

We can also compare the evolution of quantum-mechanical average spin not to the evolution of one particle according to classical mechanics, as we did throughout the paper, but rather to the evolution of an ensemble of classical particles. The fact that the limit of quantum mechanics when $\hbar \to 0$ corresponds to statistical classical mechanics was stressed already many times in the past [28] and more recently [18]. We have shown in a simple case, by considering an ensemble of classical particles initially prepared in such a way that their spins are parallel and their orbital angular momenta are also parallel, distributed according to the Poisson law (71), that the average classical results coincide, for large N, with the quantum-mechanical ones [29]. With this statistical assumption, we can interpret the collapse, the revivals, and the universal revival time of the harmonic oscillator. These results will be discussed more extensively in future works.

ACKNOWLEDGMENTS

We would like to thank Frederic Faure for numerous discussions on the evolution of coherent states as well as on the spin-orbit problem. One of us (P.R.) acknowledges the financial support from the Commission of the European Communities, Contract No ERB-CIPA-CT-92-2114, and the warm hospitality from Institute des Sciences Nucléaires, Grenoble.

APPENDIX A: GENERAL FORM OF SPIN DENSITY MATRIX

Let us start from the expansion of the coherent state

$$|\zeta\rangle = \sum_{nlm} \lambda_{nlm} |nlm\rangle \ . \tag{A1}$$

We introduce three quantities $\Lambda^{(0)}$, $\Lambda^{(1)}$, and $\Lambda^{(2)}$ as

$$\Lambda^{(0)}_{lm} = \sum_{n} |\lambda_{nlm}|^2 \ , \tag{A2}$$

$$\Lambda^{(1)}_{lm} = \sum_{n} \lambda_{nlm}\, \lambda^*_{nlm-1} \ , \tag{A3}$$

$$\Lambda^{(2)}_{lm} = \sum_{n} \lambda_{nlm}\, \lambda^*_{nlm-2} \ . \tag{A4}$$

In particular, when $m = l$, $\Lambda^{(0)}_{ll} = \Lambda_l = |\lambda_{lll}|^2$, which occurs in (68)–(70) for $m = l$. The density matrix separates into three parts: one where only $\Lambda^{(0)}$ appears, called $\rho_s^{(0)}$; one where $\Lambda^{(1)}$ appears, called $\rho_s^{(1)}$; and one where $\Lambda^{(2)}$ appears, called $\rho_s^{(2)}$:

$$\rho_s = \rho_s^{(0)} + \rho_s^{(1)} + \rho_s^{(2)} \ , \tag{A5}$$

$$\langle +|\rho_s^{(0)}|+\rangle = \sum_{lm} \Lambda^{(0)}_{lm} \left[|f_l + g_l\, m|^2 \cos^2\left(\frac{\theta}{2}\right) + |g_l\, a_-(m)|^2 \sin^2\left(\frac{\theta}{2}\right) \right] , \tag{A6}$$

$$\langle -|\rho_s^{(0)}|-\rangle = \sum_{lm} \Lambda^{(0)}_{lm} \left[|f_l - g_l\, m|^2 \sin^2\left(\frac{\theta}{2}\right) + |g_l\, a_+(m)|^2 \cos^2\left(\frac{\theta}{2}\right) \right] , \tag{A7}$$

$$\langle +|\rho_s^{(0)}|-\rangle = \tfrac{1}{2} \sin(\theta)\, e^{-i\phi} \sum_{lm} \Lambda^{(0)}_{lm}\, (f_l + g_l\, m)(f_l^* - g_l^*\, m) = \langle -|\rho_s^{(0)}|+\rangle^* \ . \tag{A8}$$

If we take into account only $\rho_s^{(0)}$, the eigenvalues are independent of ϕ. For $L = N$ one has $\rho_s^{(1)} = \rho_s^{(2)} = 0$ and the nonzero $\Lambda^{(0)}$ have $l = m$ (i.e., Λ_l instead of $\Lambda^{(0)}_{lm}$).

The density matrices $\rho_s^{(1)}$ and $\rho_s^{(2)}$ are found as

$$\langle +|\rho_s^{(1)}|+\rangle = \sum_{lm} \Lambda^{(1)*}_{lm+1}\, (f_l + g_l\, m) \times g_l^*\, a_-(m+1)\, \tfrac{1}{2} \sin(\theta)\, e^{-i\phi} + \text{c.c.} \ , \tag{A9}$$

$$\langle -|\rho_s^{(1)}|-\rangle = \sum_{lm} \Lambda_{lm+1}^{(1)*} [f_l^* + g_l^* (m+1)] \times g_l a_+(m) \tfrac{1}{2} \sin(\theta)\ e^{-i\phi} + \text{c.c.}, \quad \text{(A10)}$$

$$\langle +|\rho_s^{(1)}|-\rangle = \sum_{lm} \Lambda_{lm}^{(1)*} \left[\cos^2\left(\frac{\theta}{2}\right) (f_l + g_l\, m) \times g_l^* a_+(m-1) + \sin^2\left(\frac{\theta}{2}\right) [f_l^* - g_l\,(m-1)] g_l a_-(m) \right] = \langle -|\rho_s^{(1)}|+\rangle^* . \quad \text{(A11)}$$

One sees that $\rho_s^{(1)}$ contains ϕ in the diagonal part. $\rho_s^{(2)}$ has only nondiagonal elements, which also contain ϕ,

$$\langle +|\rho_s^{(2)}|-\rangle = \sum_{lm} \Lambda_{lm}^{(2)*} |g_l|^2 a_+(m)\, a_-(m+2) \tfrac{1}{2} \sin(\theta)\ e^{i\phi} = \langle -|\rho_s^{(2)}|+\rangle^* \quad \text{(A12)}$$

APPENDIX B: SPECIAL CASE OF THE H ATOM

Let O denote any of the spin operators s_x, s_y, or s_z. Let us calculate the average $\langle O\rangle_t$ at time t for a wave packet that is defined at time 0 as in (57), but with a restricted sum. The spatial part $|\zeta\rangle$ is supposed to contain all the partial waves l, but with $m = l$ only. Each partial wave is, moreover, associated with a single radial quantum n_l. We have then

$$|\zeta\rangle = \sum_l \lambda_{n_l ll} |n_l ll\rangle . \quad \text{(B1)}$$

In this appendix the coefficients $\lambda_{n_l ll}$ can be left arbitrary.

The states $|n_l ll\rangle$ are eigenstates of a central Hamiltonian H_0 and in general

$$H_0 |nlm\rangle = \varepsilon_{nl} |nlm\rangle . \quad \text{(B2)}$$

The full Hamiltonian contains also a spin-orbit part V_s with a radial form factor $V_0(r)$

$$H = H_0 + V_s = H_0 + V_0(r)\, (\vec{l}\cdot\vec{s}) . \quad \text{(B3)}$$

We want to prove the following theorem:

$$\langle O\rangle_t = \langle e^{iHt} O e^{-iHt}\rangle = \langle e^{iV_s t} O e^{-iV_s t}\rangle . \quad \text{(B4)}$$

The consequence of this theorem is that the reduced density matrix $\rho_s(t)$ depends only on V_s. No characteristic time associated with H_0 occurs in the average spin evolution for this restricted wave packet.

The proof remains on a recurrence on the expansion of $\langle O\rangle_t$

$$\langle O\rangle_t = \sum_n \frac{(it)^n}{n!} \langle O^{(n)}\rangle , \quad \text{(B5)}$$

where

$$O^{(0)} = O\ ,\ O^{(1)} = [H, O]\ ,\ O^{(2)} = [H, O^{(1)}]\ , \quad \text{(B6)}$$

and, more generally,

$$O^{(n)} = [H, O^{(n-1)}] , \quad \text{(B7)}$$

$$\langle O^{(n)}\rangle = \sum_{ll'} \lambda^*_{n_{l'} l'l'} \lambda_{n_l ll} [(\varepsilon_{l'} - \varepsilon_l) \times \langle n_{l'} l'l' \,|\, O^{(n-1)} + [V_s, O^{(n-1)}]\, |n_l ll\rangle] . \quad \text{(B8)}$$

It is now possible to show that both $O^{(n-1)}$ and its commutator with V_s have only diagonal elements in the restricted basis. Let us start with $O^{(1)}$ and $O^{(2)}$ by writing $O = \vec{s}$

$$O^{(1)} = [V_s, \vec{s}] = iV_0(r)(\vec{s}\times\vec{l}) . \quad \text{(B9)}$$

$O^{(1)}$ is obviously diagonal in the basis. In the same way

$$\langle n_{l'} l'l'|O^{(2)}|n_l ll\rangle = (\varepsilon_{l'} - \varepsilon_l)\langle n_{l'} l'l'|O^{(1)}|n_l ll\rangle + \langle n_{l'} l'l'|[V_s, O^{(1)}]|n_l ll\rangle . \quad \text{(B10)}$$

The commutator of $O^{(1)}$ with V_s is a polynomial of second degree in powers of l_i. It therefore has the required property. More generally, the commutator of V_s with $O^{(n-1)}$ in the restricted basis involves a polynomial of degree n in the components l_i of the orbital angular momentum as well as the radial form factor $V_0(r)^n$. Our theorem is therefore proved.

In the case of the harmonic oscillator H_0 and V_s commute. The theorem is valid for a general wave packet and the evolution of the spin averages is independent on the period of the oscillator.

Our theorem is interesting for the H atom or for a general central potential such as the nuclear Woods-Saxon potential. There it is true only for the case of special mixing (B1).

[1] J.R. Klauder and E.C.G. Sudarshan, *Fundamentals of Quantum Optics* (Benjamin, New York, 1968).

[2] J.C. Gay, D. Delande, and A. Bommier, Phys. Rev. A **39**, 6587 (1989); M. Nauenberg, *ibid.* **40**, 1133 (1989).

[3] Z. Dačic–Gaeta and C.R. Stroud, Jr., Phys. Rev. A **42**, 6308 (1990).

[4] J.A. Yeazell, M. Mallalieu, and C.R. Stroud, Jr., Phys. Rev. A **64**, 2007 (1990); J.A. Yeazell and C.R. Stroud, Jr., *ibid.* **43**, 5153 (1991); D.R. Maecher, P.E. Meyler, I.G. Hughes, and P. Ewart, J. Phys. B **24**, L63 (1991); for a review on the electronic wave packets G. Alber and P. Zoller, Phys. Rep. **199**, 232 (1991).

[5] L.G. Yaffe, Phys. Today **36** (8), 50 (1983).
[6] J. Kurchan, P. Leboeuf, and M. Saraceno, Phys. Rev. A **40**, 6800 (1989).
[7] D.C. Meredith, S.E. Koonin, and M.R. Zirnbauer, Phys. Rev. A **37**, 3499 (1988).
[8] E.T. Jaynes and F.W. Cummings, Proc. IEEE **51**, 129 (1963).
[9] P.W. Milonni, J.R. Ackerhalt, and H.W. Galbraith, Phys. Rev. Lett. **50**, 966 (1983); for a review H.I. Yoo and J.H. Eberly, Phys. Rep. **118**, 239 (1985).
[10] R. Graham and M. Höhnerbach, Z. Phys. B **57**, 233 (1984); in *Instabilities and Chaos in Quantum Optics*, Vol. 177 of *NATO Advanced Study Institute, Series B: Physics*, edited by N. B. Abraham *et al.* (Plenum, New York, 1988), p. 147.
[11] L. Bonci, R. Roncaglia, B.J. West, and P. Grigolini, Phys. Rev. Lett. **67**, 2593 (1991); Phys. Rev. A **45**, 8490 (1992).
[12] L.E. Ballentine, Phys. Rev. A **44**, 4126, (1991); **44**, 4133 (1991); **47**, 2592 (1993).
[13] J. Slosser, P. Meystre, and S.L. Braunstein, Phys. Rev. Lett. **63**, 934 (1989).
[14] J. Gea-Banacloche, Phys. Rev. Lett. **65**, 3385 (1990); Phys. Rev. A **44**, 5913 (1991).
[15] P. Rozmej and R. Arvieu, Nucl. Phys. A **545**, 497c (1992); R. Arvieu, P. Rozmej, and M. Płoszajczak, in *New Trends in Theoretical and Experimental Physics*, Predeal Summer School 1991 (World Scientific, Singapore 1992), p. 232; P. Rozmej and R. Arvieu, Acta Phys. Pol. B **25**, 759 (1994).
[16] S.G. Nilsson, Kgl. Dansk. Vid. Selsk. Mat. Fys. Medd. **29**, No. 16 (1955).
[17] For a review H. Friedrich and D. Wintgen, Phys. Rep. **183**, 37 (1989).
[18] L.E. Ballentine, *Quantum Mechanics* (Prentice-Hall, Englewood Cliffs, NJ, 1990) [this book is now available only from the author (e-mail: ballenti@sfu.ca)]; L.E. Ballentine, Yumin Yang, and J.P. Zibin, Phys. Rev. A **50**, 2854 (1994).
[19] V.V. Mikhailov, Izv. Akad. Nauk SSSR, Ser. Fiz. **37** (10), 2230 (1973) [Bull. Acad. Sci. USSR, Phys. Ser. **37**, 187 (1974)].
[20] B. Buck and C.V. Sukumar, Phys. Lett. **81A**, 132 (1981); P.L. Knight, Phys. Scr. **T12**, 51 (1986).
[21] V.V. Arnold, *Mathematical Methods of Classical Mechanics* (Springer, New York, 1978).
[22] S.J.D. Phoenix and P.L. Knight, Ann. Phys. (N.Y.) **186**, 381 (1988); Phys. Rev. A **44**, 6023 (1991).
[23] S.D. Boris, S. Brandt, H.D. Dahmen, T. Stroh, and M.L. Larsen, Phys. Rev. A **48**, 2574 (1993).
[24] This limit provides for finite N the explanation of the change of the direction of $\langle \vec{L} \rangle$. The length of this vector is however less than L.
[25] B. Edlen, in *Spectroscopie I*, edited by S. Flügge, Handbuch der Physik Vol. XXVII (Springer-Verlag, Berlin, 1964), p. 107.
[26] R.G. Littlejohn and W.G. Flynn, Phys. Rev. A **45**, 7697 (1992).
[27] H. Frisk and T. Guhr, Ann. Phys. (N.Y.) **221**, 229 (1993).
[28] A. Einstein, J. Franklin Inst., **225**, 263 (1936); M. Born, J. Phys. Radium (Paris) **20**, 43 (1959); D. Home and M.A.B. Whitaker, Phys. Rep. **210**, 223 (1992).
[29] R. Arvieu and P. Rozmej, Phys. Rev. A **50**, 4376 (1994). There are a few misprints in the sentence that follows Eq. (13) of this reference. Correct form is: under time evolution λ_l, N and x_0 are multiplied by $(-1)^{-il\omega_0 t}$, $e^{-2i\omega_0 t}$, and $e^{-i\omega_0 t}$, respectively.